A Wide Range of Te t ing Re t on an E celle t Li hi m-Ion Cell Chemi t t o be ed a Benchma k fo Ne Ba tt e Technologie

Je ie E. Ha lo ,[1,2] Xiao ei Ma,[1,2] Jing Li,[1,2] E ic Logan,[1,2] Y long Li ,[1,2] Ning Zhang,[1,2] Lin Ma,[1,2] S ephen L. Gla ie ,[1,2] Ma c M. E. Co mie ,[1,2] Ma tt he Geno e e,[1,2,*] Sam el B t ea ,[1,2] And e Came on,[1,2] Jamie E. S a k,[1,2] and J. R. Dahn [1,2,**],

[1] D A , D , H , . B3H 4 2, C
[2] D C , D , H , . B3H 4 2, C

We present a wide range of testing results on an excellent moderate-energy-density lithium-ion pouch cell chemistry to serve as benchmarks for academics and companies developing advanced lithium-ion and other "beyond lithium-ion" cell chemistries to (hopefully) exceed. These results are far superior to those that have been used by researchers modelling cell failure mechanisms and as such, these results are more representative of modern Li-ion cells and should be adopted by modellers. Up to three years of testing has been completed for some of the tests. Tests include long-term charge-discharge cycling at 20, 40 and 55°C, long-term storage at 20, 40 and 55°C, and high precision coulometry at 40°C. Several different electrolytes are considered in this $LiNi_{0.5}Mn_{0.3}Co_{0.2}O_2$/graphite chemistry, including those that can promote fast charging. The reasons for cell performance degradation and impedance growth are examined using several methods. We conclude that cells of this type should be able to power an electric vehicle for over 1.6 million kilometers (1 million miles) and last at least two decades in grid energy storage. The authors acknowledge that other cell format-dependent loss, if any, (e.g. cylindrical vs. pouch) may not be captured in these experiments.
 [DOI: 10.1149/2.0981913jes]

Manuscript submitted July 30, 2019; revised manuscript received August 16, 2019. Published September 6, 2019.

Lithium-ion cells are being used in grid energy storage and in electric vehicles where long lifetime is extremely important. At this time, many of these applications are generally not as demanding as they might seem. This is because it can be rare that cells are subjected to 100% depth of discharge cycling again and again on a daily or several times daily basis. For example, Pearre et al.[1] show that the average daily driving range for 484 gasoline vehicles in the US was 32.6 miles (52 km) and that the vast majority of daily range need is in the 0–50 mile range (0 – 80 km). For an EV with a 300 or 400 km range this represents about 25% DOD on a daily basis. Many researchers have shown that the lifetime of lithium-ion cells measured in cumulative charge throughput is much longer when low DOD duty cycles are applied (e.g.).[2,3]

This situation may change with the proposed introduction of "robo taxis", long haul electric trucks and vehicle-to-grid applications. In the former, vehicles will be driving all day, much like a conventional taxi and undergoing nearly 100% DOD cycling. Long haul trucks will almost certainly run in near 100% DOD situations. Cells in vehicles tethered to the grid will bew(angacki(lifetime)-upifetime)-ces

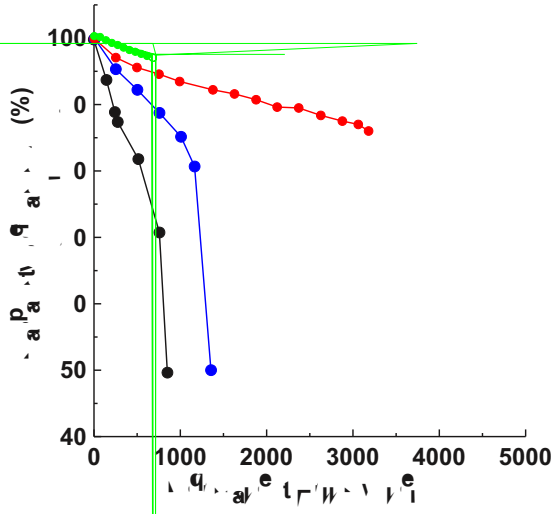
100
0
0
0
0
50
40
0
1000
2000
3000
4000
5000

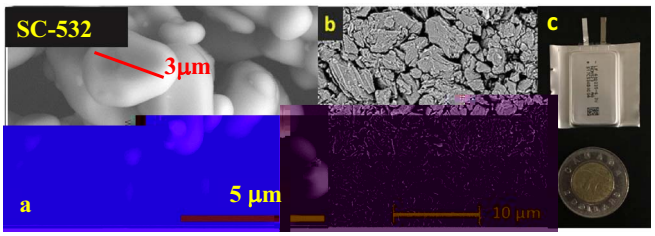

Fig e 4. a) SEM image of the single crystal NMC532 powder (SC-532); b) Top view SEM image of the AML-400 negative electrode surface after compression; c) shows an image of one of the 402035-size pouch cells next to a Canadian $2 coin (a "toonie").

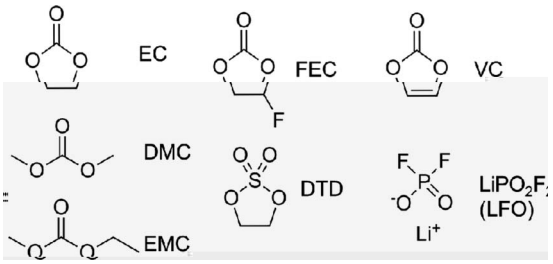

Fig e 5. Solvents and additives used in the electrolytes incorporated into the pouch cells used in this work. EC = ethylene carbonate (CAS# = 96-49-1), DMC = dimethyl carbonate (CAS# = 616-38-6), EMC = ethyl methyl carbonate (CAS# = 623-53-0), FEC = fluoroethylene carbonate (CAS# = 114435-02-8), DTD = ethylene sulfate (CAS# = 1072-53-3), VC = vinylene carbonate (CAS# = CAS No.872-36-6), $LiPO_2F_2$ (called LFO here) = lithium difluorophosphate (CAS# = 24389-25-1).

and negative electrodes consisted of 94 wt.% and 95.4 wt.% active materials, respectively. The positive electrode was compressed to 3.5 g/cm^3 and negative electrode was compressed to 1.55 g/cm^3. Prior to filling with the designed electrolytes, pouch cells were cut open and dried at 100°C under vacuum for 14 h to remove residual moisture. Afterwards, pouch cells were filled with 0.85 mL electrolyte in an Ar-filled glove box and sealed with a pouch sealer (MSK-115A Vacuum Sealing Machine) under vacuum at a pressure of −90 kPa (relative to atmospheric pressure). Figure 4a shows an SEM image of the single crystal NMC532 powder while Figure 4b shows a top view SEM image of the negative electrode surface. Figure 4c shows an image of one of the 402035-size pouch cells next to a Canadian $2 coin (a "toonie").

The cells in this work have a designed capacity of about 240 mAh at C/20. Table Ia shows the actual specific energy and energy density of the pouch cells used in this work. Even though these are very small cells where the area of the pouch is much larger than the area of the jelly roll, the specific energy is still 200 Wh/kg. The energy density is relatively low compared to that of a larger cell. To give readers some idea of the energy density that could be obtained in a larger cell, Table Ib shows the "stack energy density" for three designs which mirror what was used in the 402035 cells but with differing electrode thicknesses. The stack energy density accounts for everything except the additional volume due to the cell casing, dead space and excess electrolyte. Typically real energy densities can be 75% of the stack energy density for cells of a few Ah capacity. For example a 21700-size NMC532/graphite cell from a reputable manufacturer has a mass of 62.5 g, a volume of 24.3 cm^3 and a capacity of 3.75 Ahr when charged to 4.3 V (which is the design upper cutoff voltage for the 402035 pouch cells used here). Assuming an average voltage of 3.75 V, this corresponds to a specific energy of 225 Wh/kg and an energy density of 580 Wh/L. The energy density of this 21700 cell is 72.5% of the stack energy of the cell design used in this paper (see Table Ib).

All of the cells in this work were bar coded so that their results could be included in laboratory data bases. Although unconventional, we have included the barcodes for the cells in many of the legends of the graphs of results. This is because many of the cells discussed here are still running ongoing tests. Interested readers can contact the authors to obtain updates on one or more cells by referring to barcode numbers.

Electrolytes used.—There were several electrolytes used over the course of this work. The chemicals used in the electrolytes are shown in Figure 5. All these chemicals, plus methyl acetate (MA) and $LiPF_6$ (not shown in Figure 5), were battery grade, obtained from Shenzhen Capchem (China) and used as received.

The electrolyte solvent blends used in this work were EC:EMC 3:7 (by weight), EC:DMC 3:7 (by weight), EC:EMC:DMC 25:5:75 (by volume) and EC:EMC:MA 3:5:2 (by weight). All electrolytes used either 1.0, 1.2, 1.5 or 1.8 M $LiPF_6$ salt sourced from either BASF or

Table 1. a) Mea ed p ope ie of he NMC532/g aphi e 402035 (40 mm 20 mm 3.5 mm hick) po ch cell ed he e. The po i e elec ode a 94% ac i e ma e ial, he loading a 21.1 mg/cm^2 a ge a 21.3) and he elec ode den i a 3.5 g/cm^3. The nega i e elec ode a 95.4% ac i e ma e ial, he loading a 12.2 mg/cm^2 a ge a 11.8) and he elec ode den i a 1.55 g/cm^3. b) S ack ene g den i of he NMC532/g aphi e co ple fo e e al elec ode hickne e . b) S ack ene g den i calc la ion gi e al e fo he elec ode ack (nega i e coa ing/coppe /nega i e coa ing/ epa a o /po i i e coa ing/al min m/po i i e coa ing/ epa a o). A mp ion coppe foil = 8 µm, al min m foil = 15 µm, epa a o = 16 µm, N/P capac a io = 1.1 a 4.3 V, a e age cell o age = 3.75 V. The highligh ed o ep e en he de ign ed in hi o k.

a)

Cell designation	Average Voltage	Capacity (mAh)	Mass (g)	Volume (cm^3)	Specific Energy (Wh/kg)	Energy Density (Wh/L)	Positive areal capacity (mAh/cm^2)
403025	3.75	240	4.5	2.3	200	390	3.5

b)

Cathode loading (mg/cm^2)	Cathode active material fraction	Cathode density (g/cm^3)	Cathode reversible capacity (mAh/g)*	Cathode irreversible capacity (%)	Anode loading (mg/cm^2)	Anode active material fraction	Anode density (g/cm^3)	Anode reversible capacity (mAh/g)	Anode irreversible capacity (%)	Stack Energy Density (Wh/L)
21.3	**94**	**3.5**	**175**	**10**	**11.8**	**95.4**	**1.55**	**350**	**8**	**795**
25.0	94	3.5	175	10	13.85	95.4	1.55	350	8	815
30.0	94	3.5	175	10	16.6	95.4	1.55	350	8	836

*measured at 30°C and C/10 between 3.0 and 4.3 V.

Shenzhen Capchem. We have seen no penalty associated with lifetime reduction using the first three solvent blends, unless high rate charge (> 1C at 20°C) is attempted. The DMC containing blends are preferred due to higher ionic conductivity for high rate charge.[21] If even higher rates of charge are desired, then methyl acetate can be added as in the fourth solvent blend. Figure 6 shows the conductivity of several electrolyte systems as a function of $LiPF_6$ content at 20°C and also their temperature dependence at 1 molal. Figure 6 shows the advantage of EC:DMC over EC:EMC and the advantage of adding MA. Electrolytes with DMC are preferred over those with EMC when high rate charge or discharge is desired. Additions of MA cause a lifetime reduction for NMC/graphite cells[22] so one must realize that a trade-off between lifetime and higher rate capability is being made when MA is introduced. This trade-off is explored in this article.

The cells in this study used several electrolyte additives which have been shown previously to dramatically increase lifetimes. The combination of 2% VC + 1% DTD promoted by Li et al.,[12] the combination of 2% FEC + 1% LFO promoted by Ma et al.[16] and 1% LFO alone promoted by Ma et al.,[13] were used in the cells in this work.

Testing protocols used..—Long-term storage was performed by placing cells at various voltages in convection ovens at 20, 40 or 55°C for extended periods of time. Periodically, cells were extracted and subjected to a reference performance test (RPT) as shown in the left panel of Figure 7. The C/3 capacity, measured between 3.0 and 4.1 V at 20°C was monitored. After the RPT test, the cells were charged to the original storage voltage at C/3 CCCV (C/100 current limit) and placed back in their respective ovens.

Long-term cycle testing was performed using battery testers from Neware (Shenzhen, China). Cycling was normally between 3.0 and 4.3 V using a C/3 rate at 20, 40 and 55°C. Charging used CCCV mode with a C/20 current cutoff. Some testing was made at 20°C using 1C charge and discharge with CCCV charge to a C/20 current limit. The 1C testing also included a "rate map" with discharge currents of C/20, C/2, C, 2C and 3C where the charging currents were C/20 for the C/20 discharge cycle and 1C (with a CCCV to C/20) for all the other cycles in the rate map. The rate map protocol is shown in the center panel of Figure 7.

The difference between the average charge voltage and the average discharge voltage, ΔV, was measured and used as a measure of cell internal resistance. ΔV was calculated as shown in the right panel of Figure 7. Graphs of ΔV versus cycle number or time are used to monitor the stability of cell internal resistance. This can also be gleaned from the variation of the 3C cell capacity versus cycle number in the rate maps.

C -

. Cross sectional SEM images were taken of positive electrodes from cycled pouch cells. Cells after long duration testing were charged to 4.3 V and opened carefully in an argon-filled glove box. Circular discs of 1.1 cm diameter were punched from the positive electrode. Electrodes were rinsed with dimethyl carbonate twice before ion-milling with IB-19530CP cross-section polisher. Electrodes were milled with an Ar-ion beam for a 50 minute and 6 kV coarse step followed by a 5 minute and 6 kV fine step. SEM images were taken using a Hitachi S-4700 field emission electron microscope with a secondary electron detector. The images were obtained using an accelerating voltage of 5 kV and current of 15 uA.

Re l and Di c ion

Charge-discharge cycling results.—Figures 8 and 9 provide capacity retention versus cycle number data and normalized ΔV versus cycle number data for the NMC532/graphite cells testing between 3.0 and 4.3 V (0 – 100% SOC, Figure 8) and between 3.0 and 4.2 V (0 – 90% SOC, Figure 9). The cells tested at C/3 used 1.0 M $LiPF_6$ in EC:EMC 30:70 electrolyte with the selected additives indicated in the Figure legend while the cells tested at 1C used 1.2 M (2FEC + 1LFO) or 1.5 M (2VC+1DTD) $LiPF_6$ in EC:EMC:DMC 25:5:70 electrolyte. The duration of the testing is indicated in the legend. The appropriate data in Figure 8 was used in the comparison provided to Ecker et al's.[2] data as Figure 1. The reader should note the extremely expanded vertical scales in Figures 8 and 9, which vary from panel to panel.

Figure 8 shows that the additive blend 2% FEC + 1% LFO provides a substantial advantage at 20°C compared to 2%VC + 1% DTD. However, at elevated temperature, the situation is reversed. So the choice of additives could be application specific. In any case, the data in Figure 8 is far better than any literature data we have seen for NMC/graphite cells tested between 0 and 100% SOC. Comparing Figures 8 and 9 reveals that the main benefit of lowering the upper cutoff potential is better control of impedance growth at 20 and 40°C.

Figure 10 shows capacity versus cycle number for NMC532/graphite cells tested at 1C with rate maps and at 20°C. Figures 10a and 10b show that the cycling of these cells is incredibly impressive between 3.0 and 4.1 V with no measurable loss in 3C capacity. Figure 10c shows that when the additive mixture

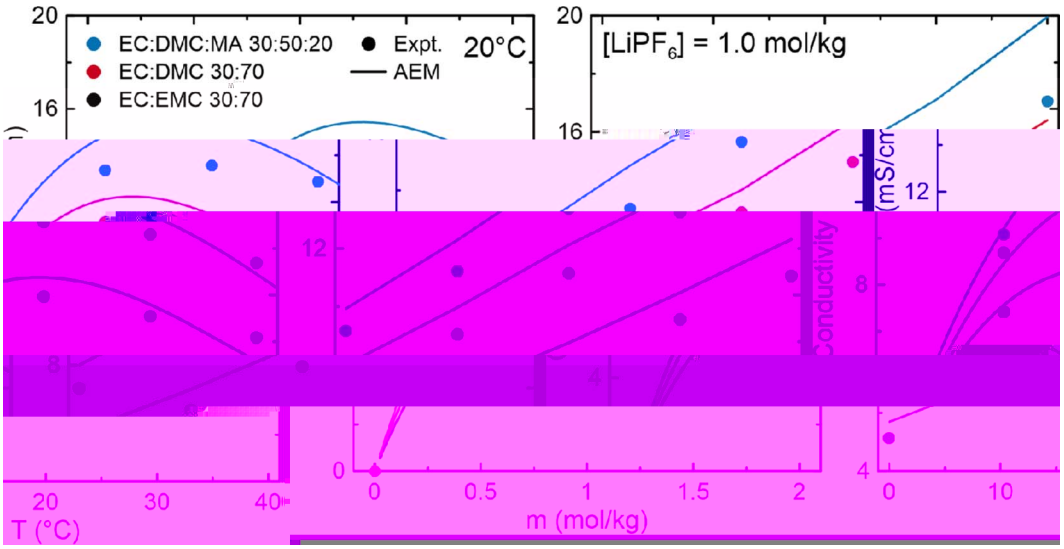

Fig e 6. a) Conductivity at 20°C versus molality in $LiPF_6$ EC:DMC:MA 30:50:20, EC:DMC and EC:EMC electrolytes. b) Conductivity versus temperature for 1.0 m $LiPF_6$ in the same solvent blends. The solid lines are the predictions of Gering's Advanced Electrolyte Model (AEM).[23]

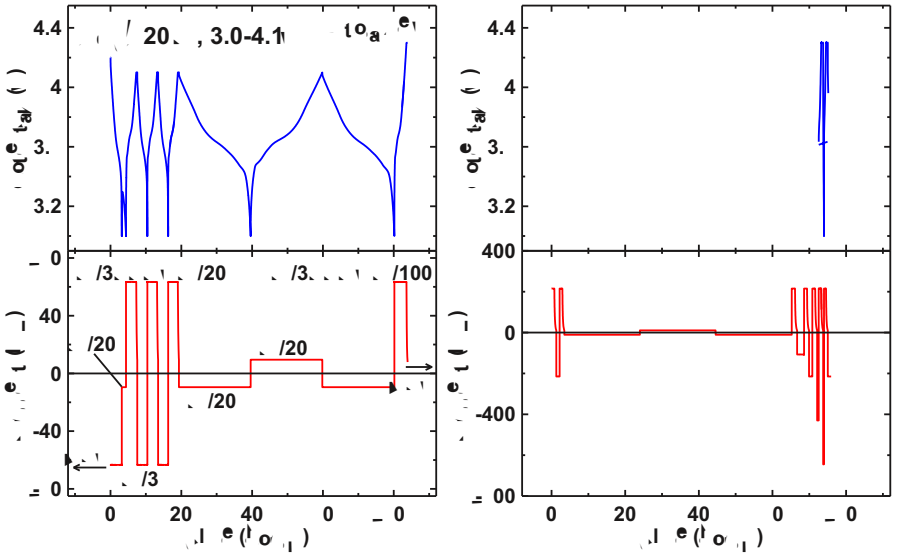
4.4
4
3.
3.2
0
40
0
-40
0
20
40
0
0
/20
/20
/20
/3
4.4
4
3.
3.2
400
0
-400
00
0
20
40
0
0

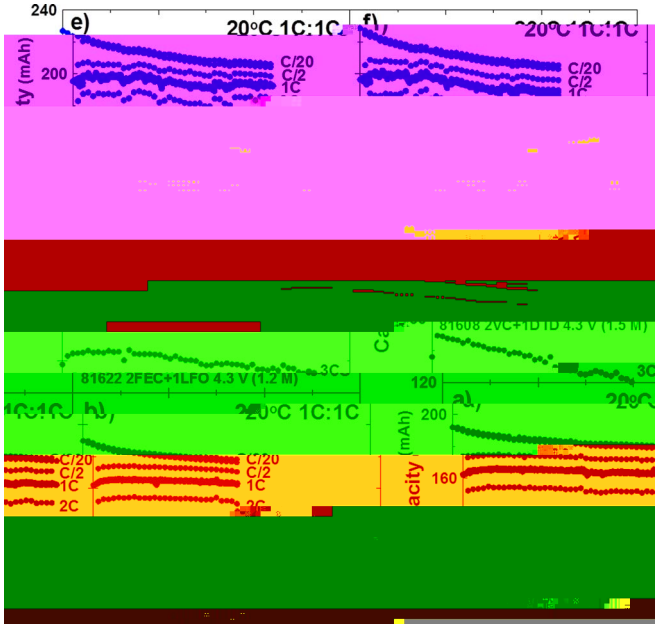

Fig e 10. Results of 1C testing of NMC532/graphite cells at 20°C with rate maps every 100 cycles. The C/20, C/2, 1C, 2C and 3C markers show the discharge capacity of the corresponding discharge at the indicated rate. a) 1.5 M $LiPF_6$ in EC:EMC:DMC 25:5:70 with 2% VC + 1% DTD tested between 3.0 and 4.1 V; b) 1.2 M $LiPF_6$ in EC:EMC:DMC 25:5:70 with 2% FEC + 1% LFO tested between 3.0 and 4.1 V; c) 1.5 M $LiPF_6$ in EC:EMC:DMC 25:5:70 with 2% VC + 1% DTD tested between 3.0 and 4.3 V; d) 1.2 M $LiPF_6$ in EC:EMC:DMC 25:5:70 with 2% FEC + 1% LFO tested between 3.0 and 4.3 V; e) 1.5 M $LiPF_6$ in EC:EMC:DMC 25:5:70 with 2% FEC + 1% LFO tested between 3.0 and 4.3 V; f) 1.8 M $LiPF_6$ in EC:EMC:DMC 25:5:70 with 2% FEC + 1% LFO tested between 3.0 and 4.3 V. Data for cells that use the 2% VC + 1% DTD additive blend are shown in black while data for cells that use the 2% FEC + 1% LFO additive blend are shown in blue.

along the capacity versus cycle number curves. Figures 11a and 11b show that there is virtually no impedance growth in the cells cycled to 4.1 V as can be determined from the virtual overlap of the 3C discharge curves for 5200 (Figure 11a) and 3100 (Figure 11b) cycles. By contrast, Figures 11c and 11d do show evidence of impedance increase when cells are charged to 4.3 V because the 3C discharge curves shift down sequentially during the cycle testing. Figures 11e and 11f show that increasing the $LiPF_6$ concentration in the presence of the 2% FEC + 1% LFO additive virtually eliminates impedance growth during cycling to 4.3 V at 3C even over 4100 cycles.

Figure 11 also can be used to determine that major cause of C/20 capacity loss in these cells is lithium inventory loss. Careful examination of the eight C/20 discharge curves in each of Figures 11a–11f shows that the portion of the curves above 3.6 V are unchanged over the duration of the cycles. This indicates no active material loss. The loss of capacity occurs only in the lower voltage region. This is caused by a shift of the negative electrode voltage-capacity curve relative to the positive electrode voltage-capacity curve due to lithium inventory loss. It will be shown later, using differential voltage (dV/dQ vs. Q) analysis that the only capacity loss mechanisms in these cells are lithium inventory loss and impedance growth, in cases where the latter occurs.

We wondered if the increase of ΔV with cycle number at 40°C and 55°C shown in Figures 8 and 9 would affect subsequent operation at 20°C. Figure 12 shows the capacity versus cycle number for NMC532/graphite cells that operated for about 1 year at 40°C or 55°C and were then moved to 20°C for continued testing for another year or so. Figures 12a and 12b show that when the cell tested at 40°C was moved to 20°C after 1000 cycles its capacity and ΔV matched those of the cell which had been cycled continuously at 20°C. Figures 12c and 12d show that when the cell tested at 55°C was moved to 20°C after 1100 cycles its capacity and ΔV were close to those of the cell which had been cycled continuously at 20°C. The capacity of the cell after moving from 55 to 20°C (shown in Figure 12c) is lower than the cell which was tested entirely at 20°C because of lithium inventory loss during the 1100 cycles at 55°C. The results in Figure 12 demonstrate this cell chemistry is extremely tolerant to extended periods at elevated temperatures.

Long-term storage testing.—Figure 13 shows the results of long-term storage testing at 20, 40 and 55°C on the NMC532/graphite pouch cells containing electrolyte with 2%VC + 1% DTD additives. Figure 13 shows these cells behave in an outstanding manner during storage testing with little loss of capacity and minor increases in ΔV. Only the cell stored at 55°C and 4.3 V for 1.3 years shows signs of troublesome capacity loss and impedance growth. The combination of the additives 2% VC + 1% DTD with this single crystal NMC/artificial graphite chemistry is simply outstanding in storage.

Figure 14 shows the results of long-term storage testing at 20, 40 and 55°C on the NMC532/graphite pouch cells containing electrolyte with 1% LFO as the additive. Figure 14 shows that these cells have an inferior storage behavior at 40 and 55°C compared to the cells with the additive blend 2%VC + 1% DTD shown in Figure 13. It is believed that the reason for this inferior behavior is the lack of an effective negative electrode SEI former like VC or FEC. Unfortunately, given the excellent performance of cells with 2%FEC + 1% LFO in Figures 8, 10 and 11, storage data for cells with 2%FEC + 1%LFO is not mature enough to report at this time. The reason for showing the data in Figure 14 is to highlight that electrolyte additives make a huge different to cell performance. The data presented in the reports on commercial cells[2,5–8,10] used for lifetime modelling do not report the details of cell chemistry, including electrolyte additives, as we do here. We examine later below the reasons for the inferior performance of the cells with 1% LFO.

Figure 15 shows the drop in voltage of the cells during 3-month open circuit storage periods plotted as a function of the storage voltage for the cells in Figures 13 and 14. The average of the voltage drop during the last four 3-month storage periods (between 0.5 and 1.3 years in Figures 13 and 14) is shown. Figure 15 shows that the voltage drops during the storage periods are very small but that they increase with both storage voltage and temperature. Cells with 2% VC + 1%DTD show smaller voltage drops (less self-discharge) than cells with 1% LFO at both 40 and 55°C. The fitted lines to the data in Figure 15 are exponential in voltage. Figure 15b shows that the data appears to be exponentially activated in voltage based on the linearity of the data when plotted with a logarithmic y-axis.

Figure 16 shows the results of storage and charge-discharge cycling tests for NMC532/graphite cells with 2%VC + 1% DTD plotted on the same graph. This is a useful comparison to see the impact of exercising the cells on lifetime. The 55°C data show similar results for cells that were cycled or stored for the 1.3 years where the test results for both are available. This suggests that the major mechanism for capacity loss at 55°C is lithium inventory loss due to a thickening negative electrode SEI. At 20 and 40°C the cells undergoing charge-discharge testing lose slightly more capacity per unit time than the corresponding cells undergoing storage testing, however their rates of impedance growth, as monitored by $\Delta V/\Delta V_o$, are very similar. As will be shown later using differential voltage analysis (dV/dQ vs. Q) the major mechanism for capacity loss in cells tested at 40°C is lithium inventory loss due to a thickening negative electrode SEI. This accelerates during cycling due to the approx. 10% volume changes of the graphite particles during lithiation and delithiation.[3] The cells at 20°C have lost only 4% capacity after 2.25 years and 3400 cycles. Differential voltage analysis does not have the resolution to determine the capacity loss mechanisms with such small capacity loss. However, by analogy to the 55°C and 40°C results it is believed the major loss mechanism is Li inventory loss at the negative electrode SEI for the cells that are cycling. This is consistent with the discussion of the C/20 capacity loss of the cells described by Figures 10 and 11.

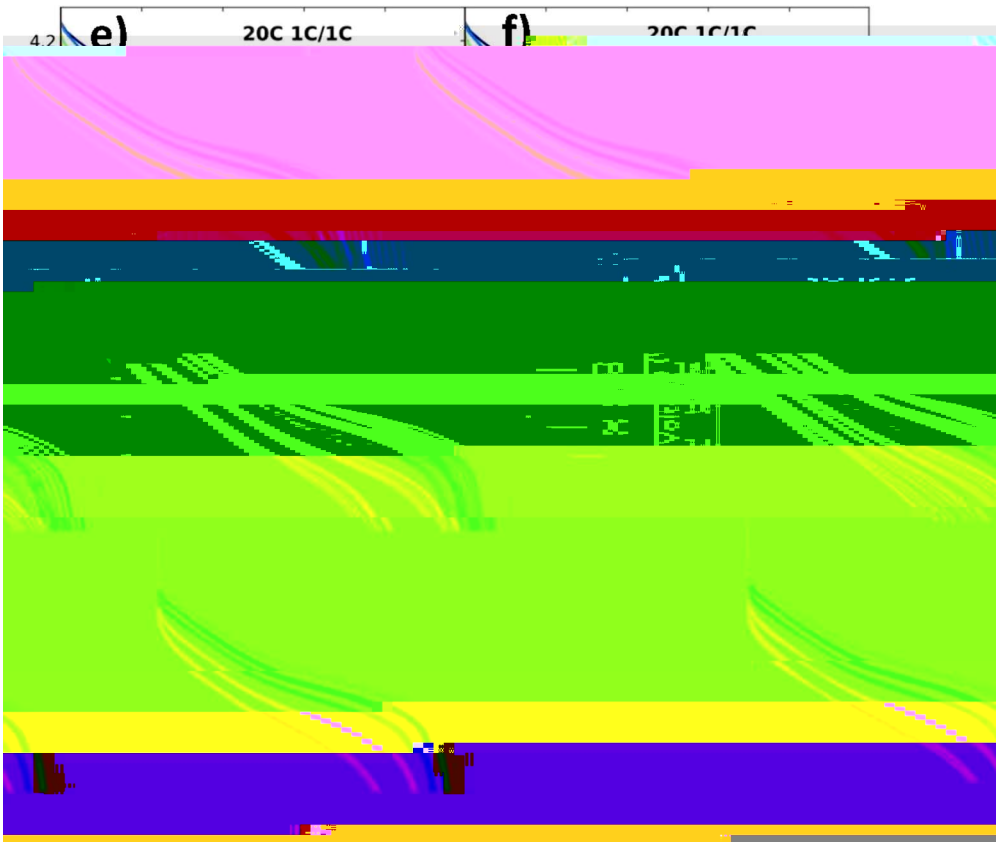

Fig e 11. Voltage versus capacity for the C/20, C/2, 1C, 2C and 3C cycles of the discharge rate maps for the cells in Figure 10. The 8 curves of each color were taken at equally spaced intervals along the capacity versus cycle number curves. a) 1.5 M $LiPF_6$ in EC:EMC:DMC 25:5:70 with 2% VC + 1% DTD tested between 3.0 and 4.1 V; b) 1.2 M $LiPF_6$ in EC:EMC:DMC 25:5:70 with 2% FEC + 1% LFO tested between 3.0 and 4.1 V; c) 1.5 M $LiPF_6$ in EC:EMC:DMC 25:5:70 with 2% VC + 1% DTD tested between 3.0 and 4.3 V; d) 1.2 M $LiPF_6$ in EC:EMC:DMC 25:5:70 with 2% FEC + 1% LFO tested between 3.0 and 4.3 V; e) 1.5 M $LiPF_6$ in EC:EMC:DMC 25:5:70 with 2% FEC +

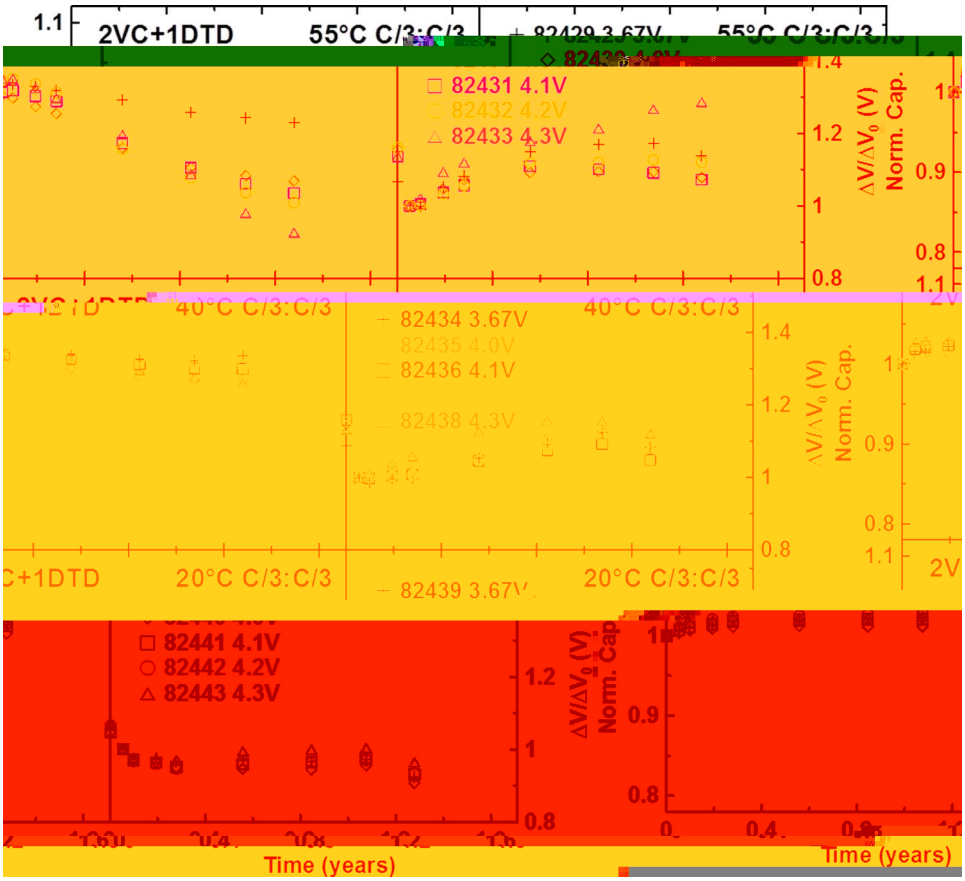

Fig e 13. Long-term storage results for NMC532/graphite cells at 20, 40 and 55°C as indicated in the legend. Storage voltages were 3.67, 4.0, 4.1, 4.2 and 4.3 V. Normalized capacity and $\Delta V/\Delta V_o$ results were obtained from RPT performed at 20°C at the times indicated. These cells contained 2% VC + 1% DTD as the additive mixture.

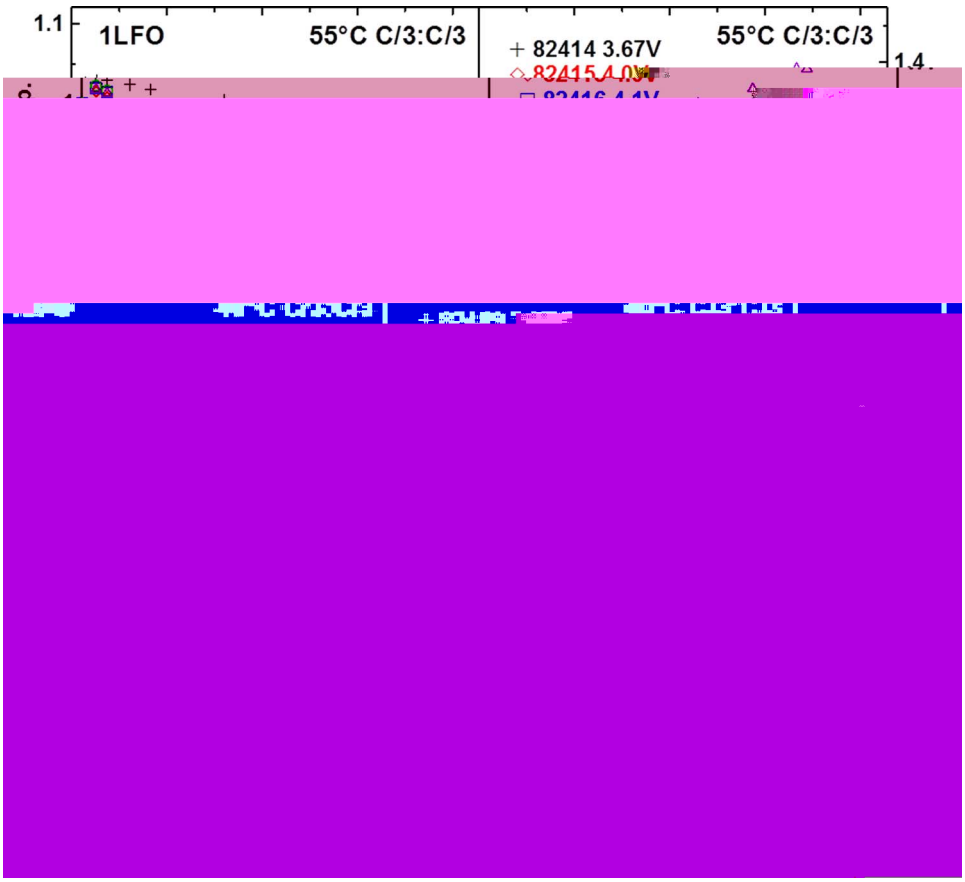

Fig e 14. Long-term storage results for NMC532/graphite cells at 20, 40 and 55°C as indicated in the legend. Storage voltages were 3.67, 4.0, 4.1, 4.2 and 4.3 V. Normalized capacity and $\Delta V/\Delta V_o$ results were obtained from RPT performed at 20°C at the times indicated. These cells contained 1% LFO as the additive.

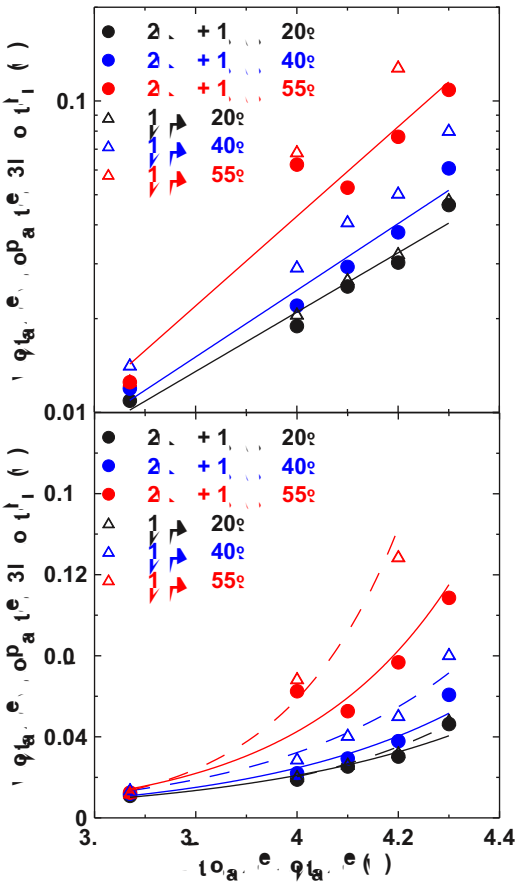
0.1
0.01
0.1
0.12
0.0
0.04
0
3.
3.
4
4.2
4.4

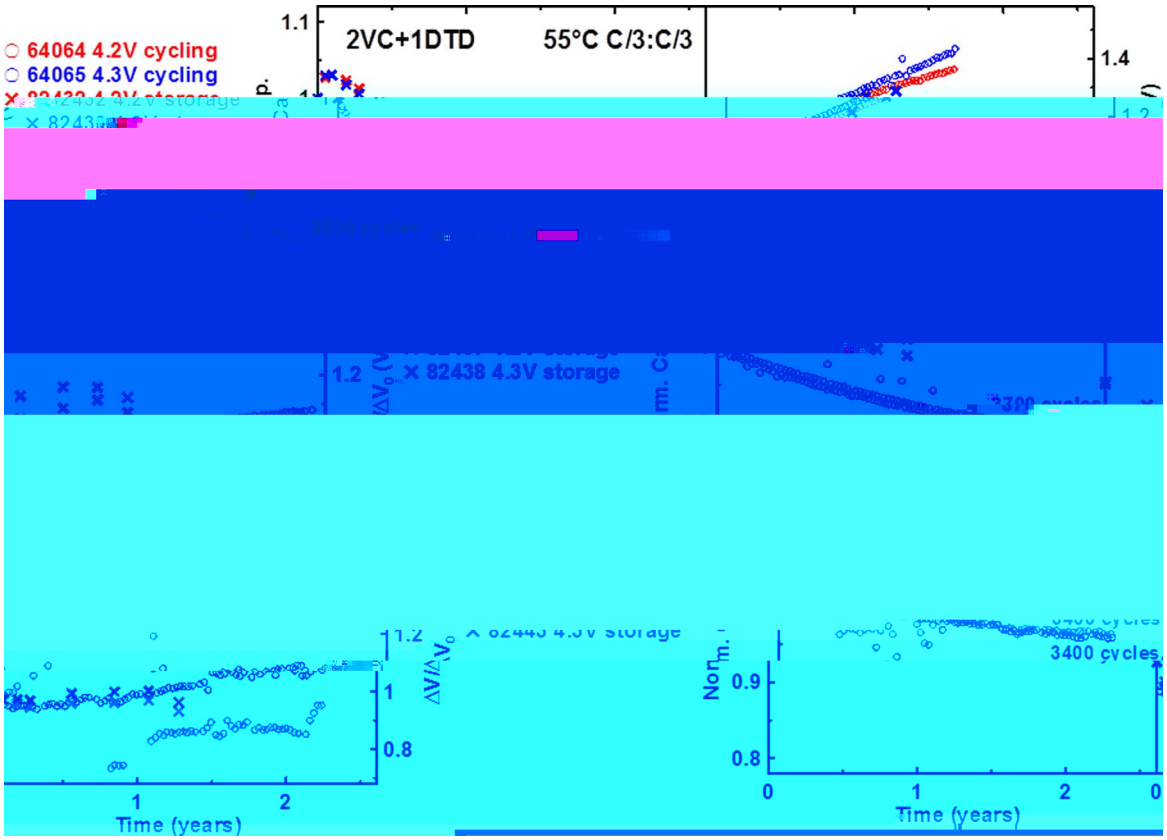

Fig e 16. Normalized capacity and $\Delta V/\Delta V_o$ plotted versus time for NMC532/graphite cells undergoing cycling or storage testing at 20, 40 and 55°C. The charge-discharge cycling was performed at C/3 between 3.0 and 4.3 V (blue circles) or between 3.0 and 4.2 V (red circles). The storage testing was done at 4.3 V (blue crosses) or at 4.2 V (red crosses). Normalized capacity for the storage testing was measured with the RPT protocol (Figure 7) at 20°C. The cells contained 2% VC + 1% DTD as additives.

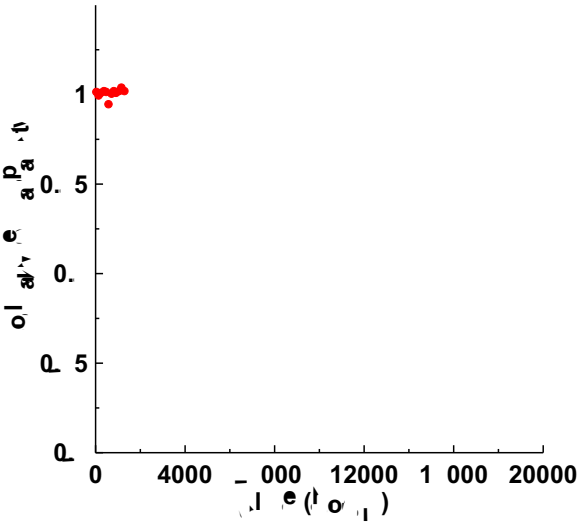

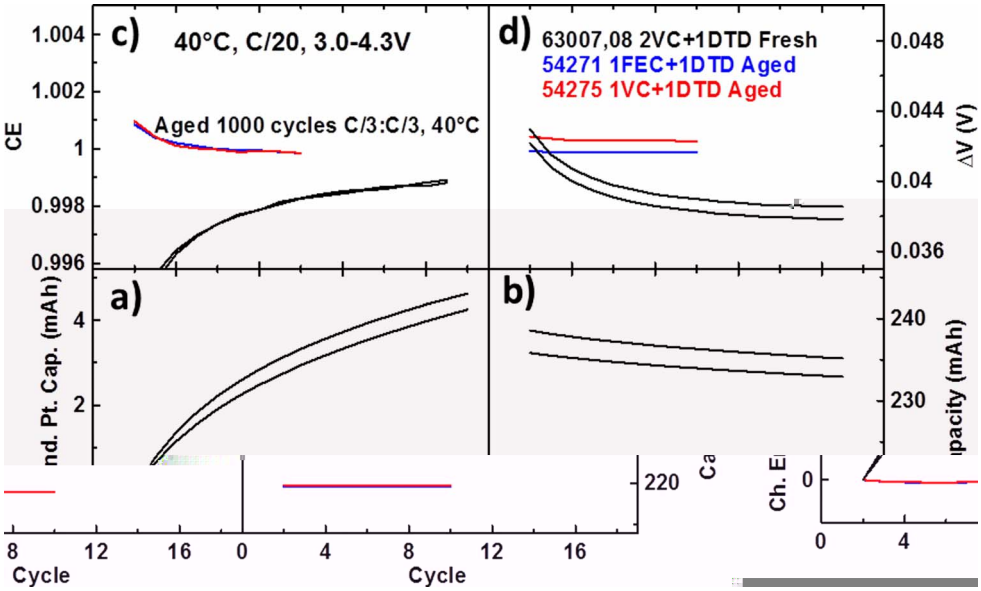

Fig e 18. Ultra high precision charger (UHPC) results for fresh and aged NMC532/graphite cells containing the electrolyte additives listed in the legend. The UHPC results were collected at 40°C between 3.0 and 4.3 V using currents corresponding to C/20. a) zeroed charge endpoint capacity; b) discharge capacity; c) coulombic efficiency (CE); and d) ΔV. Cells 54271 and 54275 were cycled 1000 times at 40°C between 3.0 and 4.3 V using currents corresponding to C/3 prior to being moved to UHPC testing. Cell 54275 was previously highlighted in Figure 12a.

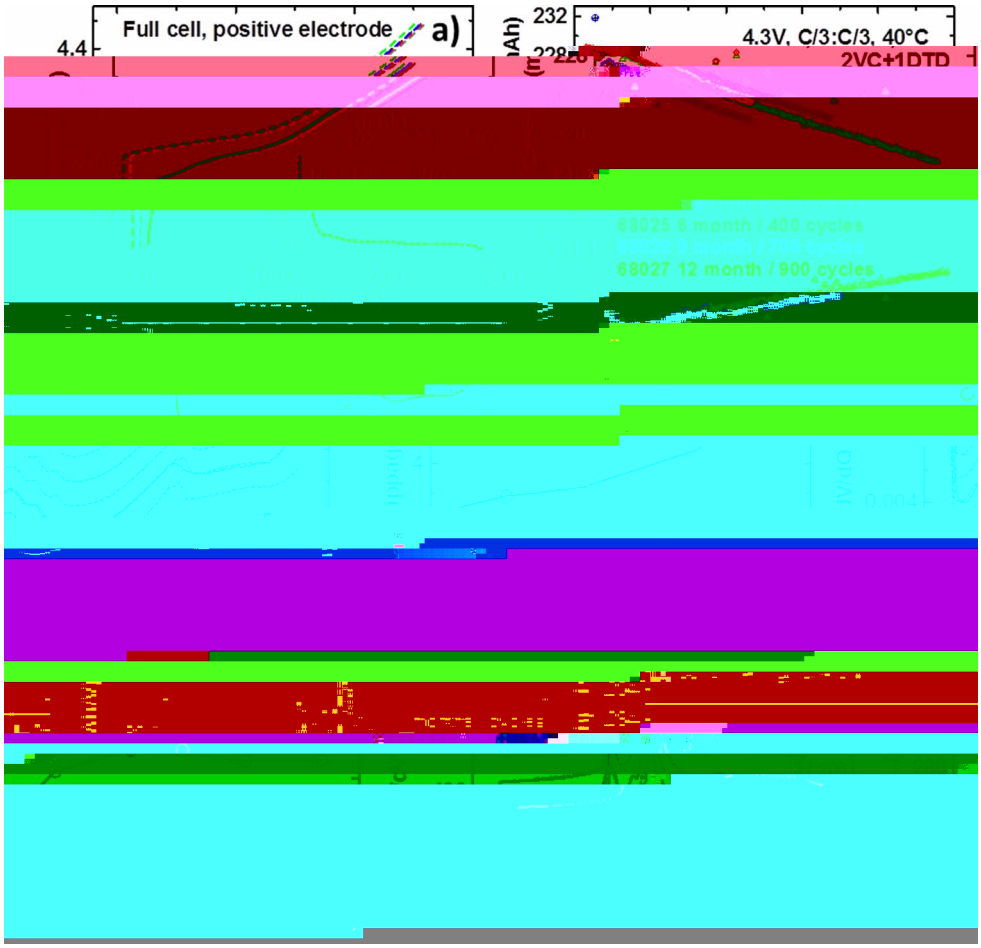

Fig e 19. Differential voltage analysis of NMC532/graphite cells tested at C/3 and 40°C between 3.0 and 4.3 V. a) the full cell voltage curves and the voltage versus capacity curves of the positive and negative electrodes versus lithium for five cells cycled 0, 200, 400, 700 and 900 times. The charge axis in Figure 18a is zero at the point where the full cell is fully discharged; b) the calculated and measured values of dV/dQ vs. Q; c) the calculated and measured values of dQ/dV vs. V; d) the cell capacity versus cycle number; e) $\Delta V/\Delta V_o$ versus cycle number; f) the relative electrode shift or slippage (due to lithium inventory loss) versus cycle number; g) the positive electrode capacity vs. cycle number; h) the negative electrode capacity versus cycle number.

performed on a more heavily cycled NMC532/graphite cell containing 2% VC + 1% DTD which was tested at 55°C (C/3 between 3.0 and 4.3 V) for 20 months. High fidelity data for dQ/dV vs V and dV/dQ vs Q was available after 0, 100 and 2500 cycles. This cell was from a different build compared to the cell considered in Figure 19. It had more excess negative electrode so it could be charged to 4.5 V without Li plating, if desired. Figure 20 shows the results of dV/dQ analysis on the cell cycled at 55°C. Figure 20 has the same format as Figure 19. Figure 20d shows that over the 2500 cycles the cell lost about 45 mAh of capacity. Figure 20e shows that over the same period the shift loss, due to Li inventory loss, was about 42 mAh, in good agreement. Figures 20f and 20g show evidence for a small loss of positive (6 mAh) and negative electrode (4 mAh) capacity, both about an order of magnitude smaller than the shift loss and hence very small. Just as the experiment considered in Figure 19, one concludes that Li inventory loss, due to thickening of the negative electrode SEI, is the major degradation mechanism for this cell. Figure 20e also shows that there is a significant impedance growth in this cell presumably due to the high temperature of operation and the 20 month duration of the test.

The volumes of gas generated in many of the cells under long-term testing were measured using Archimedes principle as described in the experimental section of reference.[22] The experiments on the cylindrical cells reported in the literature[2,5–9] give no indication of gas generated during cycling or storage. Figure 21 shows the volume of gas generated in NMC532/graphite cells during long-term cycling and storage at 20, 40 and 55°C for cells with 2%VC + 1%DTD and cells with 1% LFO as additives. As shown in Table I, the volumes of the cells themselves are 2.3 mL. Figure 21 shows that gassing is not an issue for cells cycled or stored at 20°C. Figure 21 shows that cells with 2%VC + 1%DTD undergoing continuous cycling at 40°C generate minimal gas even after 2.5 years of 100% DOD cycling. Figure 21 shows that cells with 1%LFO generate more gas than cells with 2%VC + 1%DTD under all conditions and untenable amounts of gas at 55°C. Unfortunately, comprehensive data for cells with the additive system 2%FEC + 1% LFO are not available yet. Gas generation in the cells with 2%VC + 1%DTD cycled or stored continuously at 55°C may also be problematic. It is not known what volume of gas produced in these small pouch cells would correspond to the amount needed to open the pressure activated vent in a cylindrical or prismatic cell.

The increased gassing in cells with 1% LFO stored at 40 and 55°C compared to cells with 2% VC + 1% DTD correlates well with the differences in their storage performance shown in Figures 13 and 14. Gas generation is caused by reactions between the charged electrode materials and the electrolyte. Therefore one can roughly say that when there is little gassing there are few parasitic reactions occurring in the cells. The gas volume data at 20°C suggests very few parasitic reactions and correlates well with the excellent long-term cycling of these cells at 20°C (Figures 8, 9 and 10) with little impedance growth.

Fig e 20. Differential voltage analysis of a NMC532/graphite cell tested at C/3 and 55°C between 3.0 and 4.3 V. a) the full cell voltage curves and the voltage versus capacity curves of the positive and negative electrodes versus lithium for the same cell at cycle 0, 100, and 2500. The charge axis in Figure 18a is zero at the point where the full cell is fully discharged; b) the calculated and measured values of dV/dQ vs. Q; c) the calculated and measured values of dQ/dV vs. V; d) the cell capacity versus cycle number; e) $\Delta V/\Delta V_o$ versus cycle number; f) the relative electrode shift or slippage (due to lithium inventory loss) versus cycle number; g) the positive electrode capacity vs. cycle number; h) the negative electrode capacity versus cycle number.

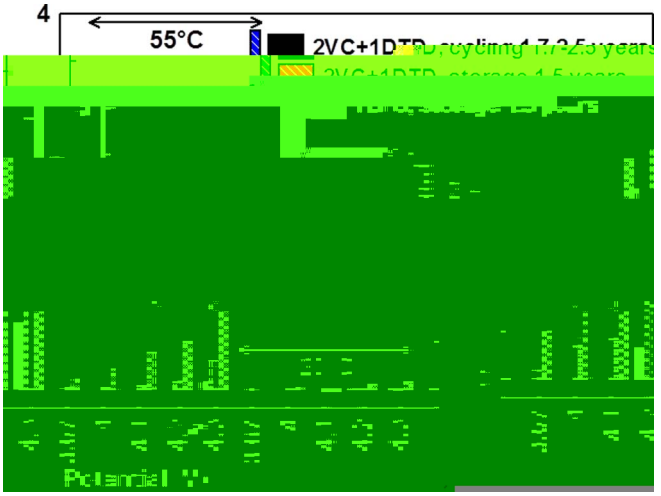

Fig e 21. Volume of gas generated during cycling and storage in the NMC532/graphite cells with electrolyte additives listed in the legend. The storage potential or the upper cutoff potential during cycling is indicated along the x-axis for the three temperatures considered: 55, 40 and 20°C. The gas bags in these cells can hold about 2.5 ml of gas before the gas begins to be compressed above atmospheric pressure. This means gas volumes measured by Archimedes principle that are greater than 2.5 mL would be even greater if the gas were at 1 atm pressure.

The small gas volumes generated at 20°C also correlate well with the excellent storage behavior of these cells at 20°C with virtually no capacity loss nor impedance growth (Figures 13 and 14).

Virtually no micro-cracking in the single crystal NMC532 electrode particles after 5000 cycles.—A cell (barcode 82306) containing the electrolyte additives 2% VC + 1%DTD was tested for 5300 cycles at 20°C using currents corresponding to 1C. The voltage limits were 3.0 to 4.1 V. The cell had 97% of its initial capacity remaining much like the results for the cell shown in Figure 10a which was tested under the same conditions. After 5300 cycles the cell was charged to 4.3 V at C/20 and then opened in a glove box. The positive electrode was cross-sectioned and imaged as described in the experimental section.

Figure 22 shows representative cross sectional SEM images of the electrode particles after 5300 cycles. No evidence of micro-cracking can be observed in particles that were initially less than 3 micrometers in size, demonstrating again the advantages of single crystal materials. This why there is no loss of positive electrode active mass in these cells during cycling. Figure 22 suggests that the cell in Figure 10a would have an incredibly long cycle life. The paper by Li et al.[31] introduces the advantages of single crystal materials compared to conventional polycrystalline positive electrode materials.

What might be the lifetime of these NMC532/graphite cells?—It is interesting to consider the possible lifetime of these cells in EV and grid storage applications. Complex models are not used here. Consider the data in Figures 10, 11 and 16. At 20°C cells can be cycled at either 1C or C/3 for 4000 100% DOD cycles with about 4% capacity loss and less than 10% impedance growth. The fractional capacity loss rate is therefore about 0.00001/cycle. At 20°C cells can be stored at full charge for 1.3 years with about 0% loss and no impedance change and at 90% charge with 0% loss and no impedance change. The capacity loss rate is 0.0/year. At 40°C, cells can be cycled at C/3 for 3700 100% DOD cycles with about 12% capacity loss and about 15% impedance growth. The fractional capacity loss rate at 40°C is about 0.000032/cycle. At 40°C, cells can be stored at full charge for 1.3 years with about 3% loss and 10% impedance change or at 90% charge with about 1.5% loss and 8% impedance change. The fractional capacity loss rate during 100% DOD storage at 40°C is about 0.02/year.

Assume a use scenario that blends storage (worst case scenario at top of charge) and cycling (worst case scenario 100% DOD) and

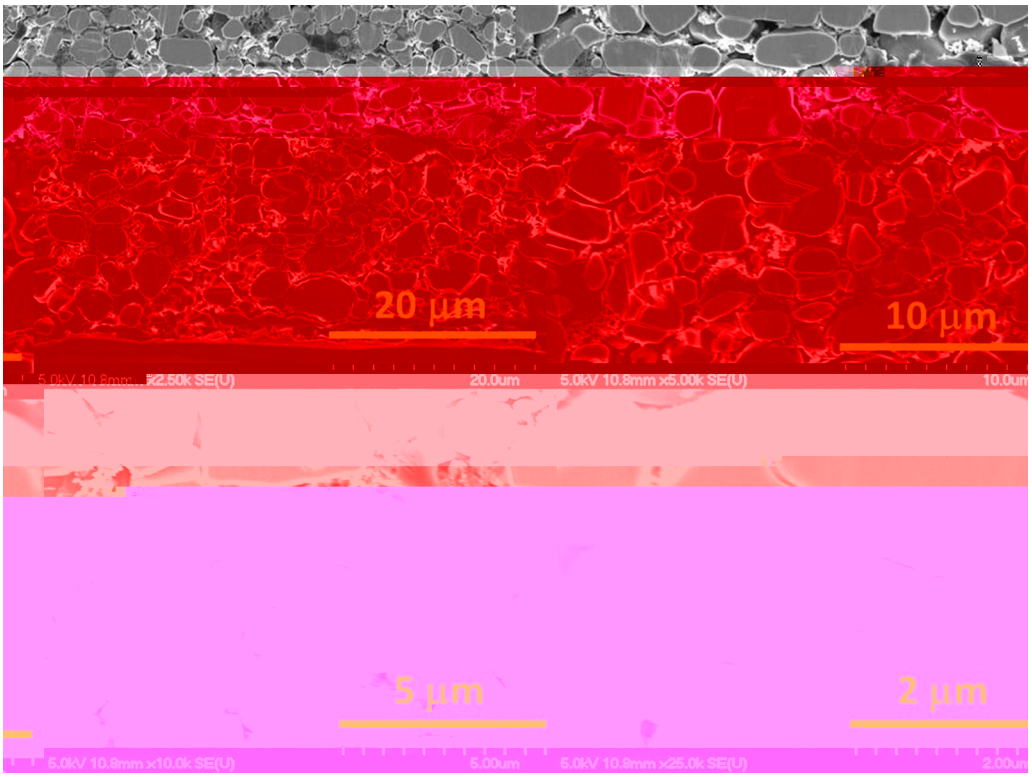

Fig e 22. Cross sectional SEM of a single crystal NMC532 positive electrode taken from a cell tested exactly under the conditions of the cell in Figure 10a. The cell had 97% capacity retention after 5300 cycles. Notice that there are virtually no microcracks in any of the electrode particles. This is why these cells show no loss of positive electrode active mass during cycling.

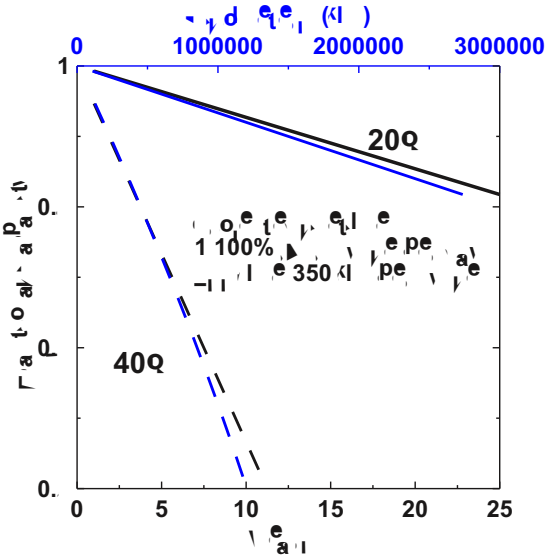

Fig e 23. Worst-case scenario lifetime and total driving range projections for the NMC532/graphite cells with 2% VC + 1% DTD at 20 and 40°C. Assumptions made were one 6 hour 100% DOD cycle per day and 350 km initial driving range per cycle. Equation 1, with M = 1, n = 3, L_c = 0.00001/cycle (20°C), L_c = 0.000032/cycle (40°C), L_s = 0.0/year (20°C) and L_s = 0.02/yr (40°C) was used to calculate Q/Q_o.

cycling in a mode where there are M 100% DOD cycles per day at an average C/n rate. That means the time of cycling each day would be 2 M n hours. The time of storage would be 24 – 2 M n. The fractional capacity as a function of time in years would be:

$$Q/Q_o = 1 - L_c\,M\,365\,t - L_s\,(24 - 2\,M\,n)\,/24\,t \qquad [1]$$

where L_c is the fractional loss per cycle, L_s is the fractional loss per year during storage and t is the time in years. This assumes that all degradation processes are linear and do not slow with time. Again, this is a worst case scenario.

Figure 23 shows the projected fractional capacity of these NMC532/graphite cells as a function of time in years in a scenario where the cells are cycled once per day (100% DOD to 4.3 V) in a cycling event that takes 6 hours. It is also assumed that during the remaining time, cells are stored at full state of charge. It is clear from Figure 23 that these cells would provide an exceptionally long total driving range in an EV if the cells were maintained at an average temperature of 20°C. Even if the cells were continually at 40°C, 10 years of lifetime to 70% capacity and a total driven distance of 1,200,000 km is projected. It is worth noting that only 3650 cycles would be required for this total driven distance and 3700 cycles have been demonstrated in Figure 16.

Most important to realize is that Figure 23 assumes 100% DOD cycling on every cycle and storage at full state of charge. If the reader reviews the literature data in Figures 1 and 2, the reader will realize that the lifetime will be much better in situations where the DOD is limited and in situations where cells are stored at lower states of charge. Admittedly, the projections in Figure 23 use the incredibly simple model described by equation 1. It is our opinion that more sophisticated models will lead to even longer lifetime projections.

Concl ion

Single crystal NMC532/graphite cells with exceptional lifetime have been developed. Storage and cycle testing up to 3 years in duration has been presented at 20, 40 and 55°C. The lifetime of these cells far exceeds that of other NMC/graphite cells reported in the literature and which have been used for lifetime modelling. It is suggested that lifetime models for NMC532/graphite cells consider the data presented here.

Full details of these cells including electrode compositions, electrode loadings, electrolyte compositions, additives used, etc. have been provided in contrast to literature reports using commercial cells. This has been done so that others can re-create these cells and use them as benchmarks for their own R+D efforts be they in the spaces of Li-ion cells or "beyond Li-ion cells".

The cells described here have two dominant failure mechanisms at 20, 40 and 55°C. These are Li inventory loss and impedance growth. We find virtually no evidence for loss of active material in these cells during cycle testing under the conditions used here.

The numeric data used in Figures with cell barcode labels indicated can be made available to interested readers. Please contact the authors.

Ackno ledgmen